Stability of MRI Turbulent Accretion Disks

Hiroyuki R. Takahashi [1] and Youhei Masada[2]

[1] Center for Computational Astrophysics, National Astronomical Observatory of Japan,
2-21-1, Osawa, Mitaka, Tokyo 181-8588, Japan
[2] Department of Computational Science, Kobe University, 1-1 Rokkodai, Nada, Kobe 657-8501, Japan
E-mail(HRT): takahashi@cfca.jp

Abstract

We study the stability of geometrically thin accretion disks with non-standard α parameter, which characterizes the efficiency of the angular momentum transport. Following recent results of numerical simulations of the Magnetorotational instability (MRI) driven turbulence, we assume that α increases with the magnetic Prandtl number. By adopting Spitzer's microscopic diffusivities, we obtain local structures of geometrically thin accretion disks consistently including effects of MRI-driven turbulence. Since the magnetic Prandtl number increases with the temperature, the efficiency of the angular momentum transport and thus viscous heating rate are smaller for a larger radius when $\delta > 0$. We found that such disks can be unstable to gravitational, thermal, and secular instabilities. It is most remarkable feature that the thermal and secular instabilities can grow in the middle part of accretion disks ($r \simeq 100 r_s$, where r_s is the Schwarzschild radius), even when the radiation pressure is negligible, while the standard Shakura & Sunyaev's accretion disk (constant α) is stable to these instabilities. We conclude that it would be difficult to maintain the steady mass accretion state unless the Pm-dependence of the MRI-driven turbulence is weak. Consideration of Pm dependence of α due to the MRI-driven turbulence may make the phase transition of accretion disks less mysterious.

Key words: accretion, accretion disks — instabilities — magnetic fields — MHD

1. Introduction

The physical mechanism for transporting the angular momentum is the important unresolved issue in accretion disks. It has been studied to understand the powerful mass accretion associated with the release of the gravitational energy by analytical and numerical procedures.

The pioneering study of the steady mass accretion into the central star and the structure of the accretion disks was done by Shakura & Sunyaev (1973) by assuming that the efficiency of the angular momentum transport is proportional to the total pressure, $t_{r\phi} = -\alpha p$, where $t_{r\phi}$ and p are the $r-\phi$ component of the stress tensor and the total pressure, respectively. α is the phenomenological dimensionless viscosity parameter, which should be determined experimentally. The disk model they developed is now referred to as 'Standard Shakura-Sunyaev Model' (see, e.g., Kato, Fukue, & Mineshige 1998, hereafter, we simply call it the 'α-model').

From the observational point of view, King, Pringle & Livio (2007) discuss that α should be of order $\simeq 0.1$ to explain the powerful energy release observed in the disk systems, such as dwarf novae, X-ray transients, and the Active Galactic Nuclei (AGNs). Since the required level of α is much larger than that obtained from the microscopic viscosity, the turbulent viscosity would be essential for the angular momentum transport in the disk systems (see, also Hartmann et al. 1998, Smak 1999, Dubus et al 2001, Starling et al. 2004, Lodato & Clarke 2004).

Balbus & Hawley (1991) studied the role of the magneto-rotational instability (MRI) in the astrophysical disk systems. The angular momentum is transported outward by the magnetic tension force. Importantly, the magnetic field is amplified due to the differential rotation even if the magnetic field strength is initially very weak. The angular momentum is transported by the amplified magnetic fields. After the discovery of the MRI, the non-linear MHD turbulence driven by the MRI has been studied as the leading mechanism for the turbulent angular momentum transport in disk systems using the numerical simulations (Hawley & Balbus 1992, Hawley 1995, Sano et al. 2004, Fromang et al. 2007). The physical properties of the MRI-driven turbulence are, however, not well determined.

A remarkable feature found in recent numerical simulations is that the efficiency of the angular momentum transport strongly depends on the magnetic Prandtl

number $Pm = \nu/\eta$ (Lesur & Longaretti 2007, Fromagn et al. 2007, Simon & Hawley 2009), where ν is the viscosity and η is the magnetic diffusivity. When the system has non-zero net magnetic flux, which would be reasonable for the astrophysical disk systems, the turbulent stress depends on the magnetic Prandtl number and the efficiency of the angular momentum transport α increases with Pm, as $\alpha \propto Pm^{\delta}$, where δ is the constant power-law index ($0 < \delta < 1$) (Fromang et a. 2007, Simon & Hawley 2009).

It should be noted that although the viscous effect suppresses the growth of MRI in the linear regime (Masada & Sano 2008, Pessah & Chan 2008), it boosts the angular momentum transport in the non-linear regime. When $Pm > 1$, the MRI grows and the angular momentum is efficiently transported. It is the central issue in the current MRI studies which should be solved to understand the gravitational energy release in the astrophysical disks.

After the findings of the Pm-dependence of the angular momentum transport, Balbus & Henri (2008) evaluated the magnetic Prandtl number in the accretion disks by assuming the fully ionized gas. They found that the magnetic Prandtl number increases with decreasing the radius r and it becomes larger than unity when $r < 100 r_s$, where r_s is the Schwarzschild radius. This result suggests that the angular momentum transport is efficient in the inner part of the disks. Considering the recent findings of the numerical studies $\alpha \propto Pm^{\delta}$, such a efficient angular momentum transport would affect the dynamics of the accretion disks.

In this paper, we construct a steady model for geometrically thin disk taking into account the effect of MRI through the parameter δ in the form $\alpha \propto Pm^{\delta}$. This should be consistent treatment of the turbulent viscosity with the results from recent local shearing box simulations (Lesur & Longaretti 2007, Simon & Hawley 2009).

This paper is organized as follows: The steady disk model with the non-standard description of the viscosity parameter $\alpha \propto Pm^{\delta}$ is constructed in § 2. We then describe the basic properties of our disk model in § 3. In § 4, we investigate the stability of our steady disk model to the gravitational, thermal, and secular instabilities. The dependence of the stability criteria on the magnetic Prandtl number (or index δ) is our interest in this section. We summarize our results in § 5.

2. Model

We construct a steady disk model taking into account the effect of the MRI-driven turbulence found in the recent local simulations (Lesur & Longaretti 2007, Simon & Hawley 2009). A fundamental assumption of this work is that the efficiency of the angular momentum transport is proportional to the magnetic Prandtl number as

$$\alpha = \alpha_0 P_M^{\delta}, \tag{1}$$

where α_0 is a constant, which should be determined so that $\alpha < 1$, and δ ranges $0 < \delta < 1$ from the result of the numerical studies (Lesur & Longaretti 2007, Simon & Hawley 2009).

In the following, we assume that the gas in the disks is fully ionized, which is reasonable for the disk of the X-ray binaries and for the inner part of the disk in AGNs. Then the viscosity ν and the electric resistivity η are estimated as

$$\nu = 1.6 \times 10^{-15} \rho^{-1} T^{\frac{5}{2}} (\ln \Lambda_{HH})^{-1} \ , \tag{2}$$

and

$$\eta = 5.55 \times 10^{11} T^{-\frac{3}{2}} \ln \Lambda_{eH} \ , \tag{3}$$

where ρ and T are the gas density and the temperature (Spitzer 1962). The Coulomb logarithms for proton-proton and electron-proton scatterings are represented above by $\ln \Lambda_{HH}$ and $\ln \Lambda_{eH}$, respectively. Then the magnetic Prandtl number is written as

$$Pm = \left(\frac{T}{4.2 \times 10^4 \ \mathrm{K}} \right)^4 \left(\frac{10^{14} \ \mathrm{cm}^{-3}}{nl} \right), \tag{4}$$

where n is the number density and $l = \ln \Lambda_{eH} \ln \Lambda_{HH}$ is the product of the Coulomb logarithms and is fixed to be $l = 40$ in the following (see, Balbus & Henri 2008).

By substituting equation (4) into (1), the efficiency of the angular momentum transport depends on the local nature of the accretion disks. The rest of the equations is the conventional ones used in the classical standard α-disk model, such as the mass conservation equation, the angular momentum conservation equation, and the energy balance between the viscous heating and the radiative cooling (see, e.g., Frank et al. 1992, Kato, Fukue, & Mineshige 1998). We assume that the gas rotates with the Keplerian speed and that the hydrostatic balance is maintained in the vertical direction. Combining these equations coupled with equations (1) and (4), we obtain the steady disk model taking into account the MRI-driven turbulence. We note that our disk model reduces to that of the conventional α-disk when $\delta = 0$.

3. Disk Structures

Figure 1 shows the radial profiles of the magnetic Prandtl number (left top), the viscous parameter α (right top), the surface density $\Sigma = 2\rho H$ (left bottom), and the temperature (right bottom), respectively. Here, ρ and H are the mass density and the scale height, respectively. The constant parameter α_0 is determined so that the maximum of α to be unity. The thick solid curves show the solutions for the standard α-disk model ($\delta = 0$),

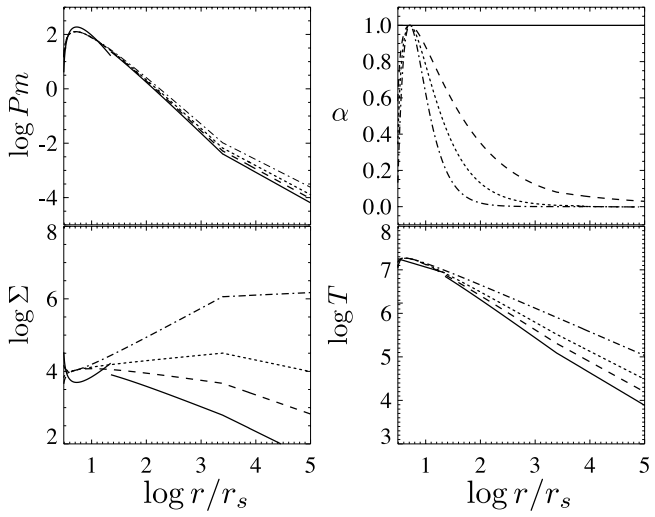

Fig. 1. Radial profiles of the magnetic Prandtl number (left top), α (right top), the surface density (left bottom), and the temperature (right bottom). α_0 is determined so that the maximum of α is unity. Thick solid curves denote the solutions for the conventional standard disk model, while dashed, dotted, and dash-dotted ones do those for $\delta = 0.25, 0.5, 1$, respectively. The other parameters are $\dot{M} = 10\dot{M}_\odot$ and $\dot{M} = \dot{M}_{\rm Edd}$

while dashed, dotted, and dash-dotted ones do those for $\delta = 0.25, 0.5, 1$, respectively. We take the mass of the central star $M = 10M_\odot$ and the mass accretion rate $\dot{M} = 10\dot{M}_{\rm Edd}$, where $\dot{M}_{\rm Edd}$ is the Eddington mass accretion rate.

As mentioned by Balbus & Henri (2008), the magnetic Prandtl number decreases with radius since the temperature decreases with it. It becomes unity around $r \simeq 100r_s$ which is qualitatively consistent with their results. In our model of non-standard α-disk models, the viscous parameter α depends on the magnetic Prandtl number through equation (1) following to the recent numerical studies. Thus, α is not uniform in space, but it steeply decreases with radius except the inner part of the disks. Since the viscosity η increases with T and the electric resistivity decreases with T, the MRI-driven turbulence is suppressed in the outer part of the disks. The gaseous materials cannot accrete inward efficiently due to the suppression of the angular momentum transport, so that the disk gas is accumulated in the outer part of the disks. It leads to the increase in the surface density compared to the standard constant α-disk models. From the consideration of the energy balance between the viscous heating and the radiative cooling, the disk temperature slightly increases.

We can see that there exists the inflection point where α rapidly decreases with decreasing the radius ($r \simeq 10r_s$). Since we adopted the zero stress boundary condition at the inner radius ($r = 3r_s$), the gaseous materials cannot rotate with the Keplerian speed inside the inner radius. The gas materials accrete onto the central star, without the influence of the turbulent viscous stress (Novikov & Thorne 1973). This results in the lower temperature and the lower efficiency of the angular momentum transport.

4. Stability Analysis

As showed in the previous section, the inclusion of the Pm-dependence in the viscous parameter α drastically changes the dynamical structure of the disk system. In this section, we show the results of the linear stability analysis of our disk model to the gravitational, thermal, and secular instabilities.

4.1. Gravitational Instability

In the previous section, we showed that the gaseous materials are accumulated in the outer part of the disks (see, Figure 1) because of the lower efficiency of the angular momentum transport. Such a mass accumulation would affect on the structure of the disks when the self-gravity of the disk gas is comparable with the gravity by the central object.

The criteria for the gravitational instability to axisymmetric perturbation is evaluated as

$$Q = \frac{\Omega c_s}{\pi G \Sigma}, \tag{5}$$

where c_s and G are the sound speed and the gravitational constant (Toomre 1964, Goldreich & Lynden-Bell 1965). When $Q < 1$, the self-gravity cannot be neglected compared to the gravity by the central star, and the gravitational instability would set in.

Figure 2 shows the radial profile of Toomre's Q-value. Solid curves show the results of standard-α disk model ($\delta = 0$), while the dashed, dotted, and dot-dashed curves show the model with $\delta = 0.25, 0.5, 1.0$, respectively. The

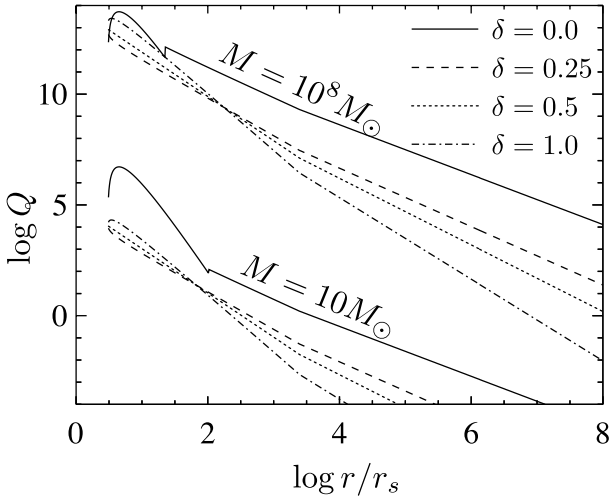

Fig. 2. Radial profiles of Toomre's Q-value. Solid, dashed, dotted, and dash-dotted curves represent for $\delta = 0, 0.25, 0.5, 1.0$, respectively. Upper four curves show the model of $M = 10 M_\odot$ (Low Mass X-ray Binaries), while lower four curves do that of $M = 10^8 M_\odot$ (AGNs).

upper four curves show the results of $M = 10 M_\odot$ (Low Mass X-ray Binaries, hereafter, LMXBs), while the bottom four curves do that of $M = 10^8 M_\odot$ (AGNs). The mass accretion rate is taken to be $\dot{M} = \dot{M}_{\rm Edd}$. We can see that the Q value decreases with radius because the gravity from the central star decreases with it. We note that the Q value decreases with increasing the index δ. As mentioned above, the efficiency of the angular momentum transport α steeply decreases with increasing δ, so that the mass is accumulated in the outer part of the disk when $\delta > 0$. Thus, the self-gravity by the accumulated mass becomes more important for a larger δ.

For LMXBs (model $M = 10 M_\odot$), the Q-value becomes smaller than unity when $r > 10^7 - 10^8 r_s$. The X-ray binaries, which are the system of the stellar mass black hole and the companion star, would be gravitationally stable since the typical size of them is much smaller than $10^8 r_s$. On the other hand, the Q-value becomes smaller than unity when $r > 10^2 - 10^3 r_s$ for the model of AGNs. This indicates that the geometrically thin disks of AGNs are gravitationally unstable, even if α is independent of Pm. The Pm-dependence of α enhances the growth of the gravitational instability due to the mass accumulation in the outer part of the disks. The self-gravity would affect the dynamical structure of the accretion disks in AGNs. Although we need to take into account the self-gravity to construct the disk model for AGNs (see, e.g., Kozlowski et al. 1979, Mineshige & Umemura 1996), it is beyond the scope of this paper. We only mention that the Pm-dependence of α enhances the growth of the gravitational instability.

4.2. Thermal and Secular Instabilities

In our models of the accretion disks with non-standard α-prescription, the viscous parameter depends on the local nature of the accretion disks through the magnetic Prandtl number (see, equations 1 and 4) following to the results of the recent numerical simulations. Thus, the viscous parameter increases with increasing the temperature, and decreases with increasing the mass density. When the gas temperature is locally increased, the viscous heating rate also increases due to the enhancement of the MRI-driven turbulence. Then the positive feedback of increasing the heating rate leads to the thermal instability. The instability criterion for the thermal instability is written as

$$\left.\frac{\partial (Q^+_{\rm vis} - Q^-_{\rm rad})}{\partial T}\right|_{\Sigma = {\rm const}} > 0 \, , \tag{6}$$

where $Q^+_{\rm vis}$ and $Q^-_{\rm rad}$ are the viscous heating rate and the radiative cooling rate, respectively. This means that the thermal instability sets in when the increasing rate of the viscous heating overcomes that of the radiative cooling. The growth rate of the thermal instability is determined by the thermal time scale.

When the gas density is locally increased, the viscous parameter α decreases. It means the suppression of the angular momentum transport. The positive feedback of this suppression leads to enhancing the mass density, resulting the secular instability. The instability criterion for the secular instability is written as

$$-\left.\frac{\partial T_{r\phi}}{\partial \Sigma}\right|_{Q^+_{\rm vis} = Q^-_{\rm rad}} < 0 \, . \tag{7}$$

This means that the instability sets in when the turbulent stress decreases when the surface density increases. The typical time scale of this instability is the viscous time scale.

For the simple treatment of two type of instabilities, we introduce two dimensionless parameters, β and γ.

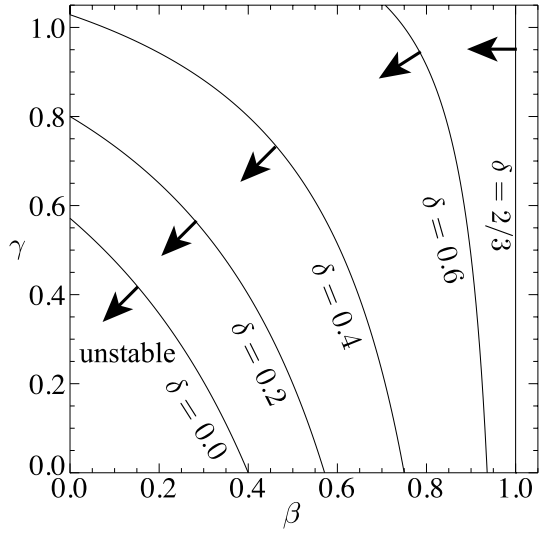

Fig. 3. Thermal and secular unstable domain on the parameter space of $\beta - \gamma$. The dominance of the electron-electron scattering for the opacity is assumed. Solid curves correspond to $\delta = 00, 0.2, 0.4, 0.6, 2/3$. The lower left region of each curve denotes the unstable domain.

The ratio between the gas pressure $p_{\rm gas}$ and the total pressure p can provide the parameter

$$\beta = p_{\rm gas}/p. \tag{8}$$

The $r - \phi$ component of the stress tensor $T_{r\phi}$ is assumed to have an general form as

$$T_{r\phi} = -2\alpha p_{\rm gas}^{\gamma} p^{1-\gamma} H \ . \tag{9}$$

We study the linear stability with the parameter space of $\beta - \gamma - \delta$ to the thermal and secular instabilities.

To perform the stability analysis, we use the fact that the dynamical time scale is much shorter than the thermal time scale and the thermal time scale is much shorter than the viscous time scale. Thus, when we study the thermal instability, we can assume that the force balance in the radial direction is maintained. Thus the gaseous motion due to the temperature perturbation is restricted in the vertical direction, so that the surface density does not change in the thermal evolution time. When we consider the secular instability, the thermal valance is maintained since the thermal time scale is much shorter than the viscous time. These assumptions can filter out the thermal and oscillatory mode and make the stability analysis easy.

When the electron-electron scattering is the dominant source of the opacity, the criteria for the thermal and secular instabilities can be described by a following equation,

$$4 - 10\beta - 7\gamma(1 - \beta) + \delta(8 + \beta) > 0. \tag{10}$$

Figure 3 shows the unstable domain on the parameter space of $\beta - \gamma$. Solid curves denote for $\delta = 0.0, 0.2, 0.4, 0.6, 2/3$. The left lower region of each curve corresponds to the unstable domain. When $\delta = 0$, the criterion for these instabilities reduces to that for the standard α-disk model (Kato, Fukue & Mineshige 1998). The last term of equation (10) comes from the effect of the MRI-driven turbulence. Note that the last term is always positive when $\delta > 0$, the effect of MRI-driven turbulence enhances the growth of the thermal and secular instabilities. Especially when the gas pressure dominates the radiation pressure ($\beta = 1$), the instability criterion is written as

$$\delta > \frac{2}{3}. \tag{11}$$

Note that the standard α-disk is always stable to these instabilities when the gas pressure dominates the radiation pressure. When we consider the Pm-dependence of α, the disk can become unstable to these instabilities. As we mentioned above, the magnetic Prandtl number increases with the temperature. Such a increase in the temperature enhances the saturation level of MRI-turbulence. This effect is included through the non-standard α-prescription in our model. The positive feedback effect of increasing the heating rate leads to the thermal instability.

5. Summary

We construct the disk model with the non-standard α-prescription according to the recent numerical simulations (Lesur & Longaretti 2007, Simon & Hawley 2009). In our model, α depends on the magnetic Prandtl number, which is evaluated by using the Spitzer's value (see, also Balbus & Henri 2008). The magnetic Prandtl number decreases with radius and becomes smaller than unity when $r > 100 r_s$. Then the viscous parameter α

becomes a function of r and it decreases with increasing radius.

Such a non-conventional α-disk can be unstable to gravitational, thermal and secular instabilities. For the gravitational instability, the disks model of LMXBs ($M = 10M_\odot$) is stable, while the model of AGNs ($M = 10^8 M_\odot$) is unstable to the instability as well as the standard accretion disks. The effect of MRI-driven turbulence facilitates the instability at which $r > 100r_s$. For the thermal and secular instabilities, the disk becomes unstable when $\delta > 2/3$ even if the gas pressure dominates the radiation pressure. In the conventional standard disks, it is well known that the disk is stable to these instabilities when the radiation pressure is negligible. However, when we consider the effect of MRI-driven turbulence, the saturation levels of the viscous parameter increases with increasing the temperature through the magnetic Prandtl number. The positive feedback of increasing the viscous heating rate leads to the thermal instabilities. Since the saturation levels of the viscous parameter decreases with increasing the mass density, the increase in the density leads to the inefficient angular momentum transport. Then the positive feedback effect results in the secular instability. Since the thermal instability develops faster than the secular instability, the accretion disks at which the MRI is well developed ($r < 100r_s$) would suffer from the thermal instability.

If the MRI plays an important role in operating the MHD-turbulence and the mass accretion in astrophysical disk systems, the steady mass accretion would not be maintained due to these instabilities. When the thermal instability develops, the increase in the temperature leads to the higher saturation level of the angular momentum transport in MRI-driven turbulence. It results in the increase in the mass accretion rate. Such a efficient mass accretion onto the central objects would cause the phase transition observed in the disk systems. Consideration of these instabilities driven by the MRI-driven turbulence would make the rapid transition of the astrophysical disk system less mysterious.

References

Balbus, S. A. & Hawley, J. F. 1991, ApJ, 376, 214

Balbus, S. A. & Henri, P. 2008, ApJ, 674, 408

Dubus, G., Hameury, J., & Lasota, J. 2001, A&A, 373, 251

Frank, J., King, A., & Raine, D. 1992, Accretion power in astrophysics., ed. Frank, J., King, A., & Raine, D.

Fromang, S., Papaloizou, J., Lesur, G., & Heinemann, T. 2007, A&A, 476, 1123

Goldreich, P. & Lynden-Bell, D. 1965, MNRAS, 130, 125

Hartmann, L., Calvet, N., Gullbring, E., & D'Alessio, P. 1998, ApJ, 495, 385

Hawley, J. F. 1995, Science, 269, 1365

Hawley, J. F. & Balbus, S. A. 1992, ApJ, 400, 595

Kato, S., Fukue, J., & Mineshige, S., eds. 1998, Black-hole accretion disks

King, A. R., Pringle, J. E., & Livio, M. 2007, MNRAS, 376, 1740

Kozlowski, M., Wiita, P. J., & Paczynski, B. 1979, Acta Astronomica, 29, 157

Lesur, G. & Longaretti, P.-Y. 2007, MNRAS, 378, 1471

Lodato, G. & Clarke, C. J. 2004, MNRAS, 353, 841

Masada, Y. & Sano, T. 2008, ApJ, 689, 1234

Mineshige, S. & Umemura, M. 1996, ApJl, 469, L49+

Novikov, I. D. & Thorne, K. S. 1973, in Black Holes (Les Astres Occlus), ed. C. Dewitt & B. S. Dewitt, 343–450

Pessah, M. E. & Chan, C. 2008, ApJ, 684, 498

Sano, T., Inutsuka, S., Turner, N. J., & Stone, J. M. 2004, ApJ, 605, 321

Shakura, N. I. & Sunyaev, R. A. 1973, A&A, 24, 337

Simon, J. B. & Hawley, J. F. 2009, ApJ, 707, 833

Smak, J. 1999, Acta Astronomica, 49, 391

Spitzer, L. 1962, Physics of Fully Ionized Gases, ed. L. Spitzer

Starling, R. L. C., Siemiginowska, A., Uttley, P., & Soria, R. 2004, MNRAS, 347, 67

Toomre, A. 1964, ApJ, 139, 1217